

Field-induced phase transitions in antiferroelectric liquid crystals

Tiezhen Qian and P. L. Taylor

Department of Physics, Case Western Reserve University, Cleveland, Ohio 44106

(Received 17 March 1999)

A theoretical study is made of the process by which an antiferroelectric smectic liquid crystal undergoes a field-induced transition to ferroelectric alignment. We find that for cells of moderate thickness the initial departure from antiferroelectric alignment occurs as a continuous Fréedericksz transition. The following transition from partial alignment to complete ferroelectric ordering may occur as either a first-order or continuous transition, depending on the relative strength of some of the model parameters. The case where the transition is continuous provides a possible mechanism for some recently observed thresholdless transitions in these systems. [S1063-651X(99)01609-8]

PACS number(s): 61.30.Cz, 64.70.Md

I. INTRODUCTION

The electric-field-induced transition between antiferroelectric (AF) smectic C_A^* (SC_A^*), and ferroelectric (F) smectic C^* (SC^*) phases in AF liquid crystals (AFLC's) constitutes the basis of tristable switching, which has shown great advantages over the bistable switching found in surface-stabilized ferroelectric liquid crystal cells in display applications [1]. This field-induced phenomenon not only exhibits the threshold and hysteresis behavior, for which it is valued in display applications, but also shows interesting phase transition kinetics, an example of which is quasi-one-dimensional fingerlike solitary-wave propagation parallel to the smectic layers [2]. The study of this field-induced transition is therefore not only necessary for display design, but is also important for physical understanding of both the phase stabilization mechanism in SC_A^* and SC^* and the nonlinear dynamical process involved in the phase transition kinetics.

A phenomenological model based on nearest-neighbor interactions between smectic layers has been proposed as a basis for the study of the various static and dynamic properties of AFLC's [3], including devil's staircases in the commensurability of the director helical structure [3], the field-induced Fréedericksz transition [4], and field- and quench-induced propagating fingers [2,3,5]. This model takes into account the elastic distortion, the effective layer-layer interaction, the coupling of local polarization with the applied field, the dielectric anisotropy, and the surface anchoring effect. In this paper, we adopt and generalize this model to investigate systematically the field-induced Fréedericksz transition and the field-induced AF- F transition. The phase sequence is explored through a free energy minimization for a moderately thin cell with surface anchoring effects included. The critical fields are obtained for the two phase transitions and the characteristics of these phase transitions are discussed.

The paper is organized as follows. In Sec. II, we generalize our model by adding an energy barrier term to the layer-layer interaction. This term will be shown to affect the order of the AF- F transition. We then reformulate our model by introducing two auxiliary angle variables, which represent the relative rotation and the mean rotation of the directors in adjacent smectic layers, respectively. This is equivalent to a

coupled model that incorporates the cooperative motion of all smectic layers rather than neglecting the molecular rotation in those layers whose initial local polarization was aligned in the direction of the applied field [4]. In Sec. III, we discuss the Fréedericksz transition. For moderately thin cells (thickness \sim several μm) and weak fields, we map the field-induced director rotation to a nematic Fréedericksz transition problem. We show that a continuous transition, characterized by a director rotating in the same sense in adjacent layers, occurs at a critical field E_F , which is shown to be inversely proportional to the cell thickness. It is also pointed out that due to the existence of a certain small but finite intrinsic length scale (~ 10 nm), it is no longer valid to map the field-induced director rotation to a nematic Fréedericksz transition problem when the cell thickness is comparable to this intrinsic length. This explains why there is a critical thickness below which continuous rotation in the same sense in adjacent layers becomes inaccessible [3,4]. In Sec. IV, we discuss the AF- F transition. We note that after the Fréedericksz transition, the same-sense director rotation quickly saturates, while a relative director rotation in adjacent layers is gradually induced by an increasing field, resulting in a weakened AF order. We find that at another critical field E_{th} , the weakened AF order becomes unstable and a transition from the AF state to the F state may be nucleated. We show that the AF- F transition can be of either first order or second order, depending on the height of the energy barrier introduced in Sec. II, with these two regions being separated by a tricritical point. For small barrier height, the transition is of second order, and this may be related to an observed feature of AF- F switching, namely, thresholdless antiferroelectricity [6]. When the barrier height is sufficiently large, there is a first-order AF- F phase transition with a pretransitional effect in the AF state. The critical field E_{th} is shown to be independent of either cell thickness or surface treatment for the practical case of a moderately thin cell. The metastability ranges of the AF and F states are calculated for $E > E_{th}$ and $E < E_{th}$, respectively. In Sec. V, we conclude this paper with a discussion of possible future improvements in our model.

II. MODEL

We begin by listing some of the parameters and variables that might be necessary to build a model capable of exhibit-

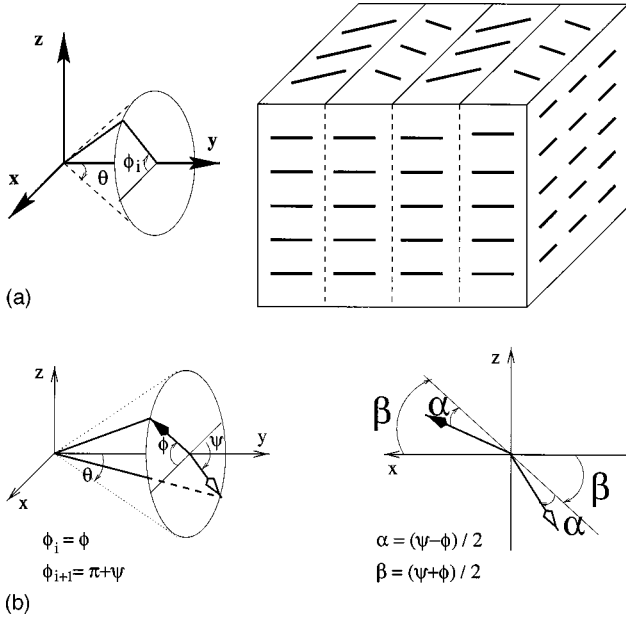


FIG. 1. (a) Geometry of the model antiferroelectric liquid crystal. (b) The two angles ϕ and ψ define the field-induced rotation of the directors in layers that were initially aligned parallel and antiparallel, respectively, to the applied field. The mean of ϕ and ψ gives the angle β that characterizes the Fréedericksz transition, while half of the difference between them gives the angle α that characterizes the AF-F transition.

ing most of the observed phenomena. We shall then discuss how various truncated models may be used to describe particular phenomena. This reduction in complexity is necessary to allow an identification of particular phenomena with specific ranges of the defining parameters in the model.

The geometry of the system is defined in Fig. 1(a). The smectic layers lie in the x - z plane and the cell surfaces lie in the x - y plane, so that the applied electric field E is in the z direction. The director \mathbf{n} in the i th layer is assumed to be confined to a cone whose surface is at an angle θ to the layer normal, and is thus completely defined by the azimuthal angle ϕ_i that the projection of \mathbf{n} onto the x - z plane makes with the x axis. The electric polarization within a layer is assumed to be of magnitude P_0 and to lie in a direction parallel to $\mathbf{n} \times \hat{\mathbf{y}}$. The local energy density of the interaction of this polarization with an applied electric field is then $-P_0 E \cos \phi_i$. An additional term in the energy density of the form $-\frac{1}{2} \Delta \epsilon \epsilon_0 \sin^2 \theta E^2 \sin^2 \phi_i$, with ϵ_0 the vacuum permittivity, is due to the dielectric anisotropy $\Delta \epsilon$. It is permissible to neglect the dielectric anisotropy when $E \ll 2P_0 / |\Delta \epsilon| \epsilon_0 \sin^2 \theta \sim 1.5 \times 10^9$ V/m. Further terms are possible when a longitudinal component of the polarization is included, but we shall neglect these in this work.

The interaction between molecules makes itself felt in several ways. Intralayer interactions are most simply represented in terms of elastic energy, and appear in the free energy density as terms of the form $\frac{1}{2} K \sin^2 \theta [(\partial \phi_i / \partial x)^2 + (\partial \phi_i / \partial z)^2]$. This is not the most general form possible, and may be inadequate at high fields, where terms quartic in $\partial \phi_i / \partial x$ and $\partial \phi_i / \partial z$ may be significant. That is, the motion of one molecule may be influenced by that of its neighbor in

a process more akin to a collision than is the force due to a Hookean spring.

Interlayer interactions are perhaps the most poorly understood component of any model of AFLC's. These presumably consist of a combination of electrostatic and steric forces with entropic effects related to small incursions of molecules into adjacent layers. For there to be a net electrostatic interaction that tends to orient a given dipole, there must be correlations in position between neighboring layers, since a uniform sheet of in-plane polarization produces no external field. Even the sign of this interaction, and hence a determination of whether this force component favors F or AF alignment, is thus a consequence of the particular nature of those correlations. In the absence of better knowledge of the interlayer forces, we assume a model in which this term is represented by some unknown function $V(\phi_{i+1}(x, z) - \phi_i(x, z))$. We then take only the first two Fourier components to be significant, and write it in the form $U \cos(\phi_{i+1} - \phi_i) - \frac{1}{2} J \cos[2(\phi_{i+1} - \phi_i)]$. A positive coefficient U favors the AF ordering, while a positive J equally promotes the AF and F ordering, but leads to an energy cost when $|\phi_{i+1} - \phi_i| \neq 0$ or π . The second-harmonic J term thereby represents an energy barrier between the AF and F ordering, and will be shown to play an essential role in determining the characteristics of the AF- F transition. In earlier treatments [2], we have included the effects of the chiral nature of the molecules by adding to the term $U \cos(\phi_{i+1} - \phi_i)$ a small term $b \sin(\phi_{i+1} - \phi_i)$. It is this addition that gives rise to the weakly helical form of the director as one passes from layer to layer. In the present treatment we neglect this term, thereby assuming that the effect of surface anchoring and applied fields are sufficient to suppress the helicity.

Finally we must include the energy of interaction of the liquid crystal with the surfaces of the cell. These anchoring terms are the most troublesome to treat theoretically because, being localized at the substrate surfaces, they are a strongly varying function of z . We shall account for them by including in the free energy a term $w_0 \delta(z \pm d/2) \sin^2 \phi_i$ with d the cell thickness, and w_0 a positive constant when the surface anchoring is planar. For polar anchoring, a further term $w_1 [\delta(z + d/2) - \delta(z - d/2)] \cos \phi_i$ must be added, but we neglect this complication in favor of a model of non-polar anchoring. With this inclusion, the working model for the free energy \mathcal{F} of the system is now $\mathcal{F} = D \sum_i \int f_i dx dz$, with D the layer thickness, and

$$f_i = \frac{1}{2} K \sin^2 \theta \left[\left(\frac{\partial \phi_i}{\partial x} \right)^2 + \left(\frac{\partial \phi_i}{\partial z} \right)^2 \right] + U \cos(\phi_{i+1} - \phi_i) - \frac{J}{2} \cos[2(\phi_{i+1} - \phi_i)] - P_0 E \cos \phi_i. \quad (1)$$

In the AF phase in the absence of an applied field, the angles ϕ_i alternate between 0 and π as one passes from layer to layer. We assume that, with our neglect of helicity, this pattern of alternation persists in the presence of applied fields. We then need consider only the values of $\phi_i(x, z)$ within two adjacent layers. All succeeding pairs of layers will then merely be a repetition of these [7]. We denote the

value of ϕ_i in all odd layers as φ and in all even layers as $\pi + \psi$. At equilibrium in the field-free AF structure we then have $\varphi = \psi = 0$.

Because the most important interactions are the interlayer forces, it is convenient to work in terms of the relative orientation of two adjacent layers. Accordingly, we define the new variables $\alpha \equiv (\psi - \varphi)/2$ and $\beta \equiv (\psi + \varphi)/2$ [see Fig. 1(b)]. The significance of the angle α is that it changes from 0 to $\pi/2$ as the ordering changes from antiferroelectric to ferroelectric. The angle β , on the other hand, characterizes the simultaneous rotation of two adjacent layers in the same direction. We shall see that it is a change of β that describes the Fréedericksz transition. In terms of these the free energy per bilayer becomes $2D \int f dx dz$, with $f = f_e + f_h + f_s$, and

$$f_e = \frac{K \sin^2 \theta}{2} \left[\left(\frac{\partial \alpha}{\partial x} \right)^2 + \left(\frac{\partial \alpha}{\partial z} \right)^2 + \left(\frac{\partial \beta}{\partial x} \right)^2 + \left(\frac{\partial \beta}{\partial z} \right)^2 \right], \quad (2a)$$

$$f_h = -U \cos 2\alpha - \frac{J}{2} \cos 4\alpha - P_0 E \sin \alpha \sin \beta, \quad (2b)$$

$$f_s = w_0 \{ [\sin^2 \alpha \cos^2 \beta + \cos^2 \alpha \sin^2 \beta] |_{z=-d/2} + [\sin^2 \alpha \cos^2 \beta + \cos^2 \alpha \sin^2 \beta] |_{z=d/2} \}. \quad (2c)$$

In the next two sections, we will show that in moderately thin cells ($d \sim$ a few μm), the Fréedericksz transition involves a continuous change in both β and α , while in the AF- F transition β is constant but α may change discontinuously.

III. FRÉÉDERICKSZ TRANSITION

In this section we investigate the Fréedericksz transition. We identify two length scales, one being intrinsic and the other field-dependent, and show that the transition occurs when the cell thickness d becomes comparable to the field-dependent length ξ_β . The critical field E_F is found to be inversely proportional to d when d is much larger than the intrinsic length scale. In this regime, the transition is continuous, and characterized by the rotation β . However, when d becomes comparable to or smaller than the intrinsic length scale, a continuous transition becomes inaccessible and a first-order AF- F transition occurs instead.

The Fréedericksz transition takes place when the applied field reaches a critical value at which the undistorted AF state becomes unstable. We start from the bulk free-energy density $f_b = f_e + f_h$, which we reduce to

$$f_b = \frac{K \sin^2 \theta}{2} [(\partial_z \alpha)^2 + (\partial_z \beta)^2] - U \cos 2\alpha - \frac{J}{2} \cos 4\alpha - P_0 E \sin \alpha \sin \beta \quad (3)$$

by assuming uniformity in the x direction. Minimization of $\int f_b dz$ yields two coupled second-order differential equations

$$K \sin^2 \theta \partial_z^2 \alpha - 2U \sin 2\alpha - 2J \sin 4\alpha + P_0 E \cos \alpha \sin \beta = 0, \quad (4a)$$

$$K \sin^2 \theta \partial_z^2 \beta + P_0 E \sin \alpha \cos \beta = 0, \quad (4b)$$

as the bulk Euler-Lagrange equations away from the two surfaces $z = \pm d/2$. From Eqs. (3) and (4a), we see that an intrinsic length scale

$$\xi_\alpha = \sqrt{K \sin^2 \theta / 4U}$$

can be defined. It is associated with the competition between elastic and interlayer forces in determining $\alpha(z)$. Using $K \sim 10^{-11}$ N, $\theta \sim 20^\circ$, and $U \sim 3 \times 10^3$ J/m³ [2], we have $\xi_\alpha \sim 10$ nm, which is of the same order of magnitude as the liquid crystal (LC) molecular length. This suggests that it will be permissible to treat α as locally determined by β if the characteristic length l over which the field-induced spatial variation of β takes place is much larger than ξ_α . Mathematically, this is equivalent to neglecting the term $\partial_z^2 \alpha$ in Eq. (4a), which leaves us with the result

$$4(U + 2J \cos 2\alpha) \sin \alpha \cos \alpha = P_0 E \cos \alpha \sin \beta. \quad (5)$$

For $E \gg U/P_0$, the only solution is $\alpha \rightarrow \pi/2$, i.e., the F state. Here we focus on the $E \ll U/P_0$ regime, which is characterized by a rotation of β with α small, i.e., a rotation in the same sense of the directors in adjacent layers, with the local AF order thus retained. Neglecting terms of higher order in α , we substitute $\sin \alpha = P_0 E \sin \beta / (4U + 8J)$ into $f_h = -U \cos 2\alpha - J/2 \cos 4\alpha - P_0 E \sin \alpha \sin \beta$, and obtain an effective homogeneous free-energy density $f_{h\beta}$ in terms of β only,

$$f_{h\beta} = -U - \frac{J}{2} - \frac{P_0^2 E^2}{8U + 16J} \sin^2 \beta, \quad (6)$$

which is correct to second order in $P_0 E / (U + 2J)$. A field-induced length scale

$$\xi_\beta(E) = \sqrt{4(U + 2J)K \sin^2 \theta / P_0^2 E^2}$$

can thus be defined to describe the elastic correlation of β . For $E \ll U/P_0$, we have $\xi_\beta \gg \xi_\alpha$, in consistency with the original condition $l \gg \xi_\alpha$ for the validity of neglecting the $\partial_z^2 \alpha$ term in Eq. (4a). This is analogous to the conventional treatment for nematic LC's; the Frank-Oseen continuum theory is applicable when the characteristic length over which elastic distortion takes place is much larger than the intrinsic LC correlation length [8].

It is readily seen that the field-induced rotation of β is equivalent to the Fréedericksz transition problem in a nematic LC cell [8]. We then rewrite the free-energy density including the surface energy,

$$f_\beta = K \sin^2 \theta (\partial_z \beta)^2 / 2 + f_{h\beta} + f_s [\delta(z + d/2) + \delta(z - d/2)] / 2,$$

in the form

$$f_\beta = \frac{P_0^2 E^2}{8U + 16J} \{ \xi_\beta^2 (\partial_z \beta)^2 - \sin^2 \beta \} + [\delta(z + d/2) + \delta(z - d/2)] w_0 \sin^2 \beta \quad (7)$$

for $P_0 E \ll U$ and $|\alpha| \ll |\beta|$. This is equivalent to the free-energy density of a nematic cell in which the substrates, lying in the x - y plane, favor homogeneous alignment in the x direction and the electric field is applied perpendicular to the

substrates (for positive dielectric anisotropy only). In this mapping, β is to be regarded as the angle the component of the nematic director in the x - z plane makes with the x axis, with $K \sin^2 \theta$ acting as the splay-bend elastic constant and ξ_β playing the role of electric coherence length. We thus obtain, in the strong anchoring limit in which $w_0 \rightarrow \infty$, the critical field $E_{F\infty}$ from the condition $d = \pi \xi_\beta$ [8], which gives

$$E_{F\infty} = \frac{2\pi}{P_0 d} \sqrt{(U + 2J)K \sin^2 \theta}. \quad (8)$$

A linear analysis similar to that employed in Ref. [9] can be easily applied to obtain Eq. (8). In Ref. [4], the critical field in the case of infinite anchoring strength was found to be

$$\mathcal{E}_F = \frac{1}{P_0} \sqrt{[2U + K \sin^2 \theta (\pi/d)^2]^2 - 4U^2},$$

which agrees with Eq. (8) for $J=0$ in the limit where $d \gg \xi_\alpha$ and thus $E_{F\infty} \ll U/P_0$. For d comparable to ξ_α , then $\mathcal{E}_{F\infty} \sim U/P_0$, which makes $\xi_\beta \sim \xi_\alpha$, and is strong enough to destroy the local AF order. Consequently, before a continuous rotation of β can happen, an abrupt jump in α occurs. This results in a critical thickness below which homogeneous nucleation of the cell becomes inaccessible [4]. The maximum β in the midplane of the cell, where $z=0$, is determined by

$$\frac{d}{2\xi_\beta} \sin \beta_M = \int_0^{\beta_M} \left[1 - \left(\frac{\sin \beta}{\sin \beta_M} \right)^2 \right]^{-1/2} d\beta, \quad (9)$$

which gives $\beta_M \propto \sqrt{E - E_{F\infty}}$ as E initially increases above $E_{F\infty}$. With $K \sim 10^{-11}$ J, $\theta \sim 20^\circ$, $U \sim 3 \times 10^3$ J/m³, $P_0 \sim 7.5 \times 10^{-4}$ C/m², and $2J/U \sim 1$ (see Sec. IV), the d -independent critical voltage $E_{F\infty} d$ is found to be ~ 0.6 V. For $d = 2$ μm , this gives $E_{F\infty} \sim 3 \times 10^5$ V/m.

To confirm this reasoning, numerical calculations were carried out, with the term of dielectric anisotropy first included in and then excluded from the expression of the free-energy functional. It is verified that there is no appreciable difference between the results obtained by including and neglecting the $\Delta\epsilon$ term. The equilibrium state is given by those values of $\alpha(z)$ and $\beta(z)$ that minimize the free-energy functional. For the fixed boundary conditions $\alpha(\pm d/2) = \beta(\pm d/2) = 0$ (i.e., in the strong anchoring limit $w_0 \rightarrow \infty$), the second-order nature of the Fréedericksz transition in moderately thin cells was verified. The numerically obtained critical field agrees well with the analytical expression in Eq. (8). For finite anchoring, the Fréedericksz transition is still continuous as long as the surface extrapolation length $l_s \approx K \sin^2 \theta w_0$ is much smaller than d . For d ranging from 1 to 10 μm , a moderately strong anchoring having $w_0 \sim 10^{-4}$ J/m² gives $l_s \approx 10$ nm, and thus suffices to keep the second-order nature of the Fréedericksz transition, as was numerically verified. In addition, the critical field E_F is still found to be approximately proportional to $1/d$, but smaller than the $E_{F\infty}$ given in Eq. (8).

In Fig. 2, the field-dependence of $\phi(0)$ and $\psi(0)$ at the midplane are shown for $d = 2$ μm , $K = 10^{-11}$ N, $U = 3.0 \times 10^3$ J/m³, $J = 1.0 \times 10^3$ J/m³, $P_0 = 7.5 \times 10^{-4}$ C/m², $\Delta\epsilon = -1.0$, $\theta = 20^\circ$, and $w_0 = 1.0 \times 10^{-4}$ J/m². It is seen

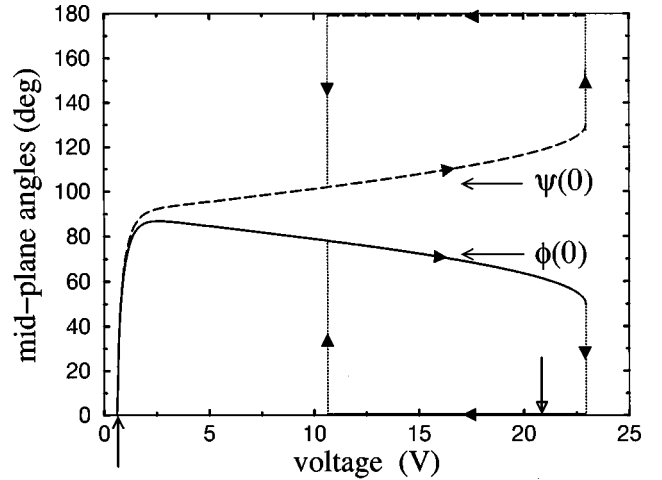


FIG. 2. Director orientations $\phi(0)$ (solid line) and $\psi(0)$ (dashed line) of alternate smectic layers are plotted as functions of applied voltage. The Fréedericksz transition occurs at $E_F d = 0.64$ V, as marked by the upward arrow. The hysteresis loop is drawn between $E_L d = 10.6$ V and $E_U d = 23.0$ V. The thermodynamic first-order transition between ferroelectric and antiferroelectric alignment occurs at $E_{th} d = 20.8$ V, as marked by the downward arrow. The parameters defined in the text used for calculation are $d = 2$ μm , $K = 10^{-11}$ N, $U = 3.0 \times 10^3$ J/m³, $J = 1.0 \times 10^3$ J/m³, $P_0 = 7.5 \times 10^{-4}$ C/m², $\Delta\epsilon = -1.0$, $\theta = 20^\circ$, and $w_0 = 1.0 \times 10^{-4}$ J/m².

that $\phi(0)$ and $\psi(0)$ undergo a transition in which they increase from zero continuously at $E = E_F$. In particular, $\phi(0)$ and $\psi(0)$ approximately exhibit a square-root dependence on $E - E_F$, as shown in the enlarged detail of Fig. 2 given in Fig. 3. The equilibrium free energy exhibits a quadratic dependence on $E - E_F$, for E close to but larger than E_F , as shown in Fig. 4, and as expected for a mean-field second-order transition. Further increasing the field induces a first-order phase transition for which the transition point and the coexistence range of the stable and metastable states are also depicted in Fig. 2. This AF-F transition will be discussed in Sec. IV.

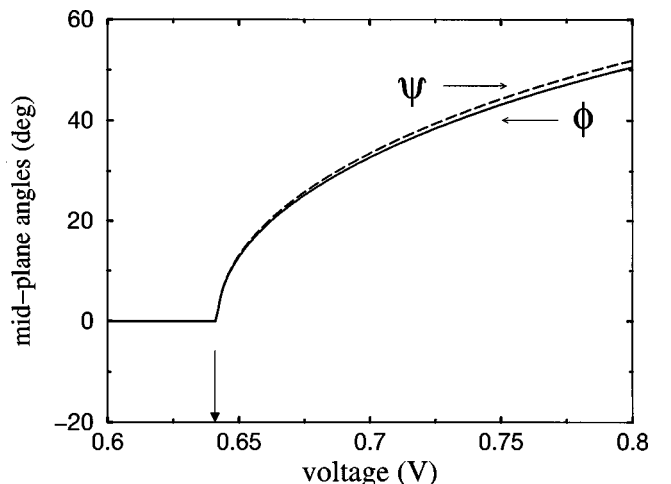


FIG. 3. This detail from Fig. 2 shows the approximate square-root dependence on $E - E_F$ for $E \geq E_F$ of the director deviations in adjacent layers.

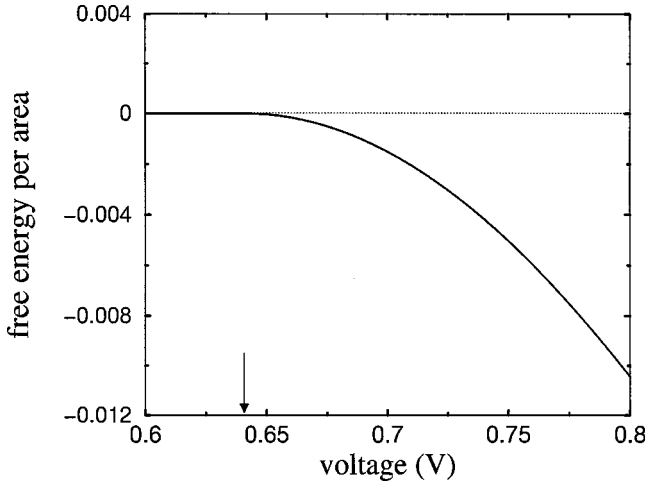


FIG. 4. Variation of total equilibrium free energy per area (in units of Ud), plotted as a function of applied voltage $V=Ed$ in the vicinity of $E_F d$. It approximates a quadratic dependence on $E - E_F$ for $E \geq E_F$. The Fréedericksz transition is noted at $E_F d = 0.64$ V.

IV. AF-F TRANSITION

For d of the order of a few micrometers, a strong enough applied field ($E \geq 5E_{F\infty}$) can cause ξ_β to be much less than d (i.e., $\xi_\beta \leq d/5\pi$). Meanwhile, for E less than or of the same order of magnitude as $U/P_0 \sim 4 \times 10^6$ V/m $\sim 15E_{F\infty}$ (for $d \sim 2$ μm), ξ_α (~ 10 nm) is less than or just comparable to ξ_β . It follows that for $\xi_\alpha \leq \xi_\beta \leq d$, the spatial variations of α and β only exist in the two boundary layers of characteristic thickness ξ_β while in the bulk $\alpha(z)$ and $\beta(z)$ are uniform, with $\beta = \pi/2$. This is confirmed in the numerical results shown in Fig. 5. It is also verified by looking at the optimal configurations that minimize the total free energy for $E \sim U/P_0$, which is of the same order of magnitude as the critical field for the AF-F transition depicted in Fig. 2. In consequence the uniform bulk has its value of α determined by the homogeneous free energy density $f_{h\alpha} \equiv f_h(\alpha, \beta = \pi/2)$,

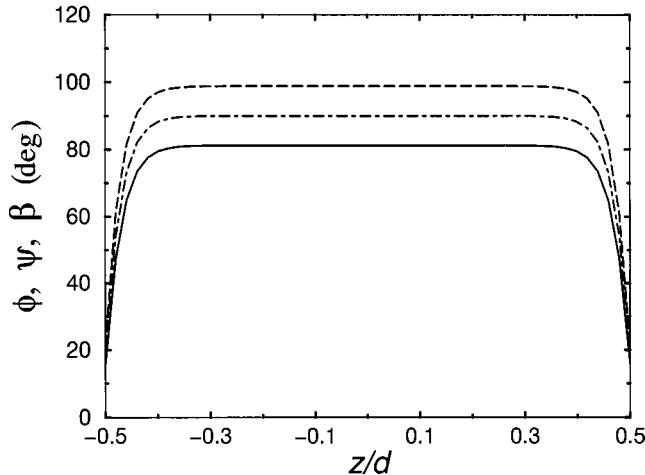


FIG. 5. Spatial variations of the director deviations ϕ (solid line), ψ (dashed line), and their mean β (dash-dotted line) for $V = Ud/P_0 = 8$ V. The parameters used for calculation are the same as those for Fig. 2.

$$f_{h\alpha} = -U \cos 2\alpha - \frac{J}{2} \cos 4\alpha - P_0 E \sin \alpha, \quad (10)$$

which determines the critical field E_{th} for the AF-F transition. Using the same parameters used for producing Fig. 2, we have verified that for $E \geq 0.4U/P_0$, minimizing $f_{h\alpha}$ gives the bulk α that is equal to the midplane $\alpha(0)$ obtained through a minimization of the total free energy. It is then obvious that E_{th} is independent of both d and the surface anchoring condition, as long as the ratio of d (\sim a few μm) to ξ_α (~ 10 nm) is of the order of 100 or larger. This agrees with experimental observations for d as small as 5 μm [5,10].

From the effective free-energy density $f_{h\alpha}$, it can be readily deduced that the change in α becomes appreciable only at $E \geq U/P_0 \gg E_F$, long after the rotation of β saturates in the bulk. Minimizing $f_{h\alpha}$ gives

$$(4U + 8J \cos 2\alpha) \sin \alpha \cos \alpha = P_0 E \cos \alpha. \quad (11)$$

For $E \ll U/P_0$, the solution $\alpha_A \approx P_0 E / (4U + 8J) \ll 1$, close to the perfect AF state $\alpha = 0$, is stable. The other two solutions, $\alpha = \pm \pi/2$, existing for arbitrary E , are required to represent two free energy maxima at $E = 0$, since deep in the AF phase, the F state is unstable for small fields [11]. This leads to the condition that $U > 2J$. Note that the original free-energy density f in Eq. (3) is invariant under the transformation $\alpha \rightarrow -\alpha$ and $\beta \rightarrow -\beta$. Here we work with $\beta = \pi/2$ and $E \geq 0$, and thus the state with $\alpha_F = \pi/2$ is lower in energy than that having $\alpha = -\pi/2$, which always corresponds to an energy maximum. For $E \geq U/P_0$, $\alpha_F = \pi/2$, a perfect F state, is the only stable solution. However, whether there is a first-order transition connecting the nearly AF state ($E \ll U/P_0$) and the perfect F state ($E \geq U/P_0$) is not obvious. In the absence of the barrier J term, there are two solutions, $\alpha = \arcsin(P_0 E / 4U)$ and $\alpha = \pi/2$ for $0 \leq E < 4U/P_0$, and only one solution, $\alpha = \pi/2$ for $E \geq 4U/P_0$. The solution at $\arcsin(P_0 E / 4U)$ is stable for $0 \leq E < 4U/P_0$ while that at $\pi/2$ is stable for $E > 4U/P_0$. At $E = 4U/P_0$, a second-order phase transition occurs, with $\partial f_{h\alpha}(\alpha = \pi/2) / \partial \alpha = 0$ and $\partial^2 f_{h\alpha}(\alpha = \pi/2) / \partial \alpha^2 = 0$. Hence there is no first-order transition for $J = 0$, since the increasing field just turns the AF state into the F state continuously. The presence of the J term therefore becomes physically necessary to explain the observed first-order nature of the AF-F transition.

The condition for the existence of a first-order phase transition can be readily derived from Eq. (11). First, we note that the number of solutions of Eq. (11) varies with E . We first consider the case where $J \leq U/10$. For $E > E_L$, where $E_L \equiv (4U - 8J)/P_0$, there is only the solution $\alpha_F = \pi/2$. For $0 \leq E \leq E_L$, on the other hand, there is an additional solution α_A . For small E , we find $\alpha_A \approx P_0 E / (4U + 8J)$. Consequently, there is always only one stable state, being either α_A when $E < E_L$ or $\alpha_F = \pi/2$ when $E > E_L$. At $E = E_L$, again the second-order transition from α_A to α_F occurs. In the case where $J > U/10$, however, the situation is quite different. For $0 \leq E < E_L$, there are two solutions, $\alpha_F = \pi/2$ and a further solution α_A . For $E_L \leq E < E_U$, where $E_U \equiv 4(U + 2J)^{3/2} / 3^{3/2} P_0 J^{1/2}$, there is a third solution, which we call α_B . This solution takes on the value $\pi/2$ when $E = E_L$, and decreases as E is increased above E_L . As E reaches E_U , the

two solutions α_B and α_A merge to a single value, $\arcsin\sqrt{(U+2J)/12J}$, which we call α_M . The physics underlying the above appearance and disappearance of solutions is clear. For $0 \leq E < E_L$, α_A is the only stable state, and $\alpha_F = \pi/2$ is an energy maximum. As E reaches E_L , $\partial^2 f_{h\alpha}(\pi/2)/\partial\alpha^2$ vanishes. After that, a metastable state α_F appears. Somewhere between E_L and E_U , at a critical field E_{th} there is a first-order transition when the energy of the state at α_F becomes equal to that at α_A . After this α_F becomes the new stable state and α_A becomes metastable. As E reaches E_U , the state at α_A becomes absolutely unstable.

We have already derived the coexistence range $E_L < E < E_U$ of the stable (metastable) α_A state and the metastable (stable) α_F state for $J > U/10$. The critical field E_{th} can be derived by solving for α_A in Eq. (11) and equating $f_{h\alpha}(\alpha_A)$ to $f_{h\alpha}(\alpha_F)$. Under the condition $U/10 < J < U/2$, the solution α_A of $(4U + 8J \cos 2\alpha)\sin \alpha = P_0 E$ is given by

$$\alpha_A = \arcsin\left(-\frac{(1-i\sqrt{3})(U+2J)}{4^{4/3}JR} - \frac{(1+i\sqrt{3})R}{6 \cdot 2^{1/3}}\right), \quad (12)$$

which exists for $0 \leq E \leq E_U$, where R is given by

$$R = \left[-\frac{27P_0E}{16J} + i\sqrt{4\left(\frac{3U+6J}{4J}\right)^3 - \left(\frac{27P_0E}{16J}\right)^2}\right]^{1/3},$$

with $\arg(R) \in [\pi/6, \pi/3]$ and α_A then being real. It can be shown that $\partial^2 f_{h\alpha}(\alpha_A)/\partial\alpha^2 > 0$ for $0 \leq E < E_U$ and that $\alpha_A = 0$ at $E = 0$. Together with the fact that $\partial^2 f_{h\alpha}(\pi/2)/\partial\alpha^2 > 0$ for $E > E_L$, these relations indicate that there is a first-order phase transition between α_A and α_F . The critical field E_{th} is determined by the equation

$$\begin{aligned} -U \cos 2\alpha_A(E_{th}) - \frac{J}{2} \cos 4\alpha_A(E_{th}) - P_0 E_{th} \sin \alpha_A(E_{th}) \\ = U - \frac{J}{2} - P_0 E_{th}, \end{aligned} \quad (13)$$

where $\alpha_A(E_{th})$ is given by Eq. (12) at E_{th} . At the tricritical point $J = U/10$, we find that $E_L = E_U$, and $\alpha_A = \alpha_F$ at $E = E_L$.

In Fig. 6, the free-energy densities of the α_A and α_F states for $U = 4J$ are plotted as functions of E in their respective stable and metastable ranges. The existence of the first-order phase transition is noted. In Fig. 7, the discontinuity in α at the transition point, given by $\alpha_F - \alpha_A(E_{th})$, is plotted as a function of J/U . In Fig. 8, the three fields E_L , E_{th} , and E_U (in units of U/P_0) are plotted as functions of J/U .

The existence of the tricritical point $J = U/10$, at which the first-order AF- F transition becomes second order, implies that the order of transition may be tuned by varying the ratio of barrier height to energy difference, J/U . This may be related to thresholdless antiferroelectricity, a term used to describe the observed continuous change from the AF state to the F state [6]. From the V-shaped characteristic transmittance-voltage curves, it was conjectured by Inui *et al.* [6] that with a diminished barrier separating SC_A^* and SC^* , the azimuthal angles ϕ_i and ϕ_{i+1} in adjacent layers may become uncorrelated. As a result, ϕ_i may vary ran-

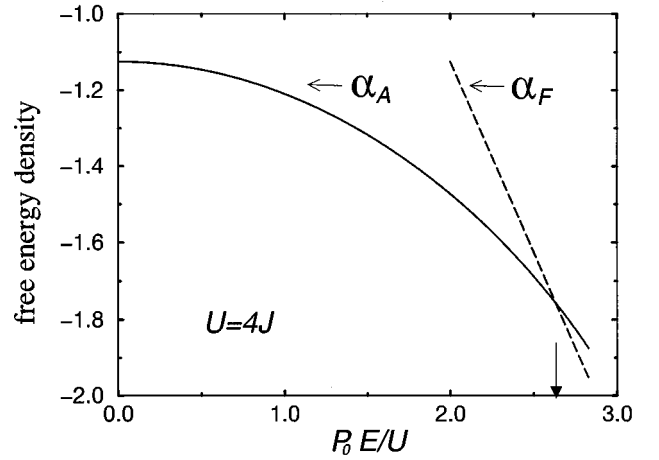


FIG. 6. Variations of minimized free energy density $f_{h\alpha}$ (in units of U) for the antiferroelectric ($0 \leq E < E_U$) and ferroelectric ($E_L < E < E_U$) states, plotted as functions of E at $U = 4J$. The first-order transition is marked by the arrow at $E_{th} = 2.63U/P_0$.

domly from layer to layer, and the effect of an applied field would be to establish gradually the SC^* order. In fact, the term ‘‘thresholdless antiferroelectricity’’ was originally introduced for this randomization of azimuthal angle variation from layer to layer [6]. Here we see another possibility: while the low-field state is still of conventional AF order, the change from AF to F ordering can be continuous if the parameter J is sufficiently small. More generally, the electric polarization can either vary continuously over the entire range of applied fields, or may have a discontinuity whose magnitude depends on the parameters of the model.

V. CONCLUSION

In summary, we have studied the two electric-field-induced transitions, i.e., the Fréedericksz transition and the AF- F transition, in a model which takes into account the intralayer elastic distortion, the nearest-neighbor interlayer interaction, the coupling of spontaneous polarization with applied field, and the surface anchoring. We find that for

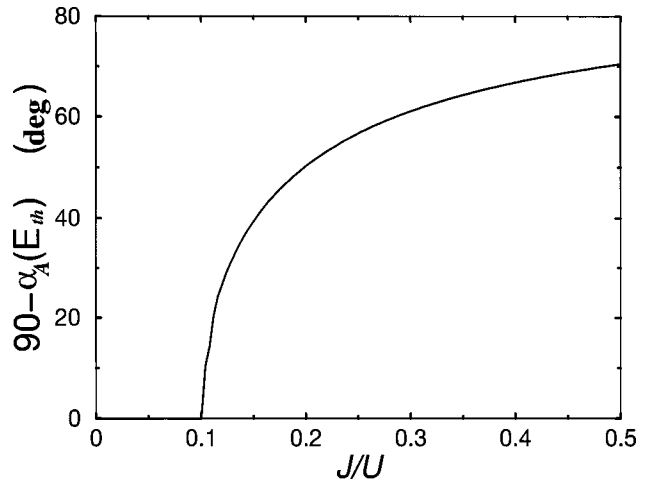


FIG. 7. The discontinuity in the relative orientation of adjacent smectic layers at the thermodynamic transition is plotted as a function of J/U for $2J < U$.

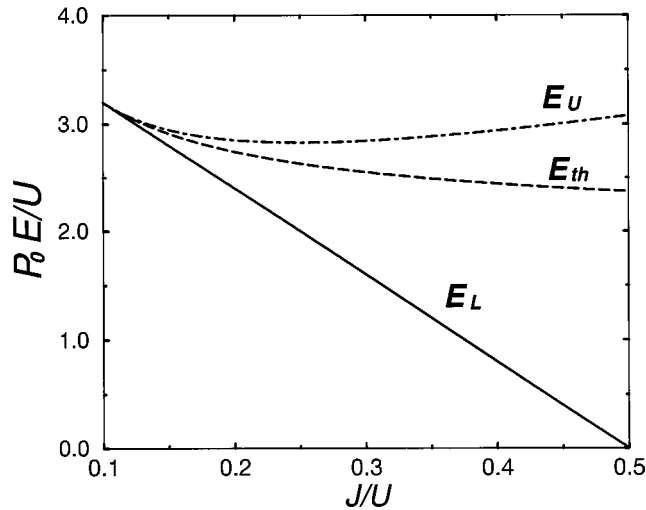


FIG. 8. Critical electric fields (in units of U/P_0) are shown as functions of J/U for $2J < U < 10J$. The solid line denotes E_L (the lower limit of metastability of the F phase), the dashed line denotes the thermodynamic transition at E_{th} , and the dash-dotted line denotes E_U (the upper limit of metastability of the AF phase).

moderately thin cells, the Fréedericksz transition, characterized by a director rotation in the same sense in adjacent layers, occurs at a critical field that is inversely proportional to the cell thickness, while the AF- F transition, characterized by opposite director rotations in adjacent layers, occurs at another much higher critical field which is independent of the cell thickness. We show that the Fréedericksz transition is of second order, while the AF- F transition can be either first order or second order, depending on the relative height of the free energy barrier separating SC^* and SC_A^* . This suggests a mechanism for the crossover from tristable

F -AF- F switching [1] to continuous V-shaped switching, i.e., thresholdless antiferroelectricity [6].

To conclude this paper, we point out that our model could be improved in a number of ways. In the present model, the only control parameter is the ratio of J to U , as only the first two harmonics are incorporated in the interlayer interaction. Including higher harmonics should make the model qualitatively and quantitatively more correct. Second, U , J , and P_0 are treated as field-independent material constants. However, it has been shown experimentally that the spontaneous polarization in AFLC's is only $\sim 10\%$ of that estimated on the assumption that all the permanent molecular dipoles are perfectly aligned [12]. Because $pE \sim 0.1k_B T$ (when $p \sim 3 \times 10^{-29}$ C m is the molecular dipole moment and $E \sim 10^7$ V/m), the spontaneous polarization is expected to be field dependent, and it may further lead to a field-dependent interlayer interaction. Finally, it has been experimentally observed that a large spatially alternating spontaneous polarization, parallel to the LC molecular tilt plane, exists in the layer-layer boundaries [13]. This longitudinal polarization could lead to an electric-field-dipole coupling quite different from that caused by the transverse spontaneous polarization perpendicular to the molecular tilt plane. It remains to be seen how significant these additional factors may be in altering the qualitative nature of the phenomena that we have modeled in this paper.

ACKNOWLEDGMENTS

We thank C. Rosenblatt, X.Y. Wang, and S. Zhang for helpful discussions, and A.M. Rudin for his contribution to the analysis. This work was supported by the National Science Foundation Science and Technology Center for Advanced Liquid Crystalline Optical Materials (ALCOM) through Grant No. DMR89-20147.

-
- [1] A. D. L. Chandani, T. Hagiwara, Y. Suzuki, Y. Ouchi, H. Takezoe, and A. Fukuda, *Jpn. J. Appl. Phys.* **27**, L729 (1988); A. D. L. Chandani, E. Gorecka, Y. Ouchi, H. Takezoe, and A. Fukuda, *ibid.* **28**, L1265 (1989).
- [2] J. F. Li, X. Y. Wang, E. Kangas, P. L. Taylor, C. Rosenblatt, Y. Suzuki, and P. E. Cladis, *Phys. Rev. B* **52**, R13 075 (1995).
- [3] X. Y. Wang and P. L. Taylor, *Phys. Rev. Lett.* **76**, 640 (1996).
- [4] X. Y. Wang, T. Kyu, A. M. Rudin, and P. L. Taylor, *Phys. Rev. E* **58**, 5919 (1998).
- [5] X. Y. Wang, J. F. Li, E. Gurarie, S. Fan, T. Kyu, M. E. Neubert, S. S. Keast, and C. Rosenblatt, *Phys. Rev. Lett.* **80**, 4478 (1998).
- [6] S. Inui, N. Imura, T. Suzuki, H. Iwane, K. Miyachi, Y. Takanishi, and A. Fukuda, *J. Mater. Chem.* **6**, 671 (1996).
- [7] J. Fournier and B. Verweire, *Ferroelectrics* **213**, 159 (1998).
- [8] P. G. de Gennes and J. Prost, *The Physics of Liquid Crystals* (Oxford University Press, New York, 1993).
- [9] F. Lonberg and R. B. Meyers, *Phys. Rev. Lett.* **55**, 718 (1985).
- [10] H. Takezoe, J. I. Lee, A. D. Chandani, E. Gorecka, Y. Ouchi, and A. Fukuda, *Ferroelectrics* **114**, 187 (1991).
- [11] In the discussion of the AF- F transition, the natural unit for E is U/P_0 . Here $E=0$ should be regarded as $E/(U/P_0) \rightarrow 0$, i.e., a field large enough to induce a uniform bulk state with $\beta = \pi/2$, but still much smaller than U/P_0 . This requires the cell thickness to be as large as several micrometers.
- [12] A. Fukuda, Y. Takanishi, T. Isozaki, K. Ishikawa, and H. Takezoe, *J. Mater. Chem.* **4**, 997 (1994).
- [13] K. Miyachi, J. Matsushima, Y. Takanishi, K. Ishikawa, H. Takezoe, and A. Fukuda, *Phys. Rev. E* **52**, R2153 (1995); D. R. Link, J. E. MacLennan, and N. A. Clark, *Phys. Rev. Lett.* **77**, 2237 (1996).